IEEE Access
Multidisciplinary | Rapid Review | Open Access Journal

Received March 19, 2020, accepted April 25, 2020, date of publication April 28, 2020, date of current version May 19, 2020.

Digital Object Identifier 10.1109/ACCESS.2020.2990992

Holographic Zoom System With Large Focal Depth Based on Adjustable Lens

DI WANG[1,2], CHAO LIU[1,2], NAN-NAN LI[1], AND QIONG-HUA WANG[2]
[1]School of Instrumentation and Optoelectronic Engineering, Beihang University, Beijing 100191, China
[2]Beijing Advanced Innovation Center for Big Data-Based Precision Medicine, Beihang University, Beijing 100191, China

Corresponding author: Qiong-Hua Wang (qionghua@buaa.edu.cn)

This work was supported by the National Natural Science Foundation of China under Grant 61927809, Grant 61805130, and Grant 61805169).

ABSTRACT In this paper, we propose a holographic zoom system based on two adjustable lenses. Different from the traditional holographic system, a digital conical lens and a liquid lens are used as the zoomable lenses. The liquid lens with large effective image aperture is designed and produced by a 3D printer. By mechanically controlling the curvature of the liquid-liquid surface, the focal length of the liquid lens can be changed easily. Compared with the other lenses, the conical lens has a larger focal depth. By encoding the phase information of the conical lens on the liquid crystal on silicon, the focal length and focal depth of the conical lens can be adjusted easily. The liquid lens and conical lens cooperate with each other so as to realize the high quality of holographic zoom projection. With such a system, the size and depth of the reconstructed image can be changed easily according to the requirement. Experimental results verify the feasibility of the proposed system.

INDEX TERMS Liquid crystal on silicon, holographic projection, lens.

I. INTRODUCTION

As a portable projection way, micro-projection technology has received more and more attention [1], [2]. In the traditional micro-projection system, the size and position of the projected image can be adjusted only by changing the distances between different solid lenses. The computer-generated holographic technology can completely record and reproduce all information of the object, and the complex amplitude information of the object can be easily adjusted by encoding the corresponding grayscale image on the liquid crystal on silicon (LCoS) [3]–[5]. Therefore, micro-projection technology based on the computer-generated holography has gradually attracted widespread attention.

In 2013, a lensless zoomable holographic projection was proposed by calculating different sampling rates [6]. By using a speckle reduction method in the process of hologram calculation, the speckle noise can be suppressed effectively. However, the magnification of the projection system is restricted by the sampling frequency. In 2016, holographic multi-projection method was proposed based on the pixel separation algorithm [7]. By using the random phase-free method and the iterative method, multiple different images can be projected on different screens at the same time. In 2018, a magnified holographic projector was introduced by combining four methods, such as the spatial division and image splicing methods [8]. The magnification of the reconstructed image by using the spatial division method or the image splicing method is affected by the spatial bandwidth product of the LCoS. Besides, other algorithms have also been proposed to adjust the size of the holographic reproduction [9]–[11]. In order to magnify the projected image optically, various adaptive lenses have been proposed in recent years [12]–[17]. Some researchers proposed a holographic projection system with optical zoom [18]. By controlling a liquid crystal lens and a Fresnel lens simultaneously, the optical zoom function can be achieved easily. However, the quality of the reconstructed image is affected by the aberration and dispersion. Compared with the liquid crystal lens, the liquid lens has the advantages such as polarization independence, large aperture, and reasonable mechanical stability [19]–[21]. In 2014, two liquid lenses were produced and used together with a Fresnel lens, then the holographic projection system with optical zoom function can be realized [22]. In 2018, an optical see-through head mounted display was proposed by using a commercial liquid lens [23]. It can be seen that liquid lens

The associate editor coordinating the review of this manuscript and approving it for publication was You Yang.

has played important roles in holographic technology due to these unique advantages.

In this paper, we propose a holographic zoom system based on two adjustable lenses. The key innovation of the proposed system is the combination of the liquid lens and digital conical lens to realize the holographic reconstruction with the zoom function, large focal depth and high quality at the same time, which can greatly promote the application of the holography. The liquid lens with special structure is designed and produced by a 3D printer. By mechanically controlling the curvature of the liquid-liquid surface, the focal length of the liquid lens can be changed easily. Then the size and depth of the reconstructed image can be changed easily by loading the corresponding phase of the conical lens on the LCoS and adjusting the focal length of the liquid lens. The proposed system has the following advantages: 1) In the traditional holographic projection systems, when the receiving screen is not in the focal plane of the system, the reconstructed image usually becomes unclear. But the proposed system has the large focal depth, so the reconstructed image can still be seen clearly in the focal depth range even if the position of the receiving screen changes. 2) A liquid lens based on the mechanical control is designed, which is produced by the 3D printer and has the reasonable mechanical stability. The proposed liquid lens has the advantages of larger aperture compared with the liquid crystal lens. Besides, compared with the commercial liquid lens, the liquid lens has the lower cost, which is expected to be mass-produced and applied in widespread of fields. In Section 4, we verify the advantages and feasibility when the proposed system is used in the holographic AR display. 3) By using the proposed system, holographic zoom projection with large focal depth can be realized. In other words, the proposed system can not only achieve the zoom function on the premise of keeping the position of the receiving screen unchanged, but also keep the reconstructed image clear even if the position of the receiving screen changes. The traditional system cannot realize the two functions at the same time. The proposed system does not require any mechanical adjustment of the optical path to achieve the zoom effect, and this feature also has great advantage in holographic near-eye display application. 4) The system is very simple and easy to operate. By using the digital conical lens, the reproduced image can be separated from the zero-order light caused by the pixel structure of the LCoS. So, the zero-order diffraction light can be eliminated easily without any diaphragms or other 4f filters. Moreover, the proposed system can be used for holographic chromatic aberration compensation. In Section 4, the structure of the color holographic system is proposed. We can see that the chromatic aberration compensation and color zoom function can be realized easily by using the designed system.

II. STRUCTURE AND OPTERATING PRINCIPLE

Figure 1 is the schematic diagram of the proposed system. It consists of a laser, a filter, a solid lens, a beam splitters (BS), an LCoS, a computer, a liquid lens and a receiving screen.

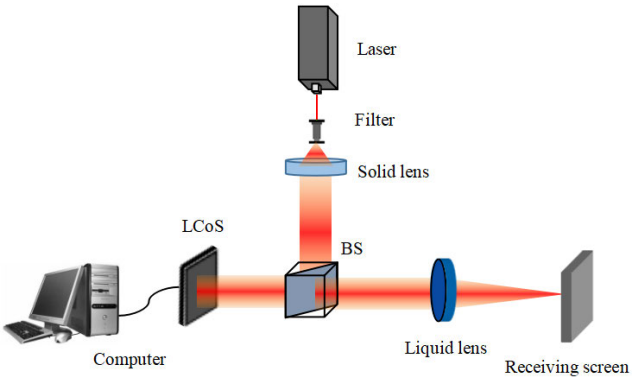

FIGURE 1. Schematic diagram of the proposed system.

The laser, filter and the solid lens can generate the collimated light. By loading the phase information of the conical lens on the LCoS, the LCoS can be used to realize the function of the digital conical lens. The BS is used to reflect the collimated beam onto the LCoS. The computer is used to generate the hologram and load the hologram onto the LCoS. When the beam illuminates on the hologram, the diffracted light passes through the BS and the liquid lens in sequence. In the proposed system, the liquid lens and the digital conical lens are used as the core components to realize the zoom function. By adjusting the effective focal length of the system, the reproduced image can be seen on the receiving screen clearly.

In order to realize the zoom function, a digital conical lens and a liquid lens are used as two adjustable lenses. Fig. 2 shows the principle of the conical lens. The conical lens has the unique advantages such as both long focal depth and high horizontal resolution, while the traditional optical lens cannot have the advantages. The phase of the conical lens φ_c is expressed as follows:

$$\phi_c = \frac{\pi}{\lambda} \frac{x^2 + y^2}{f_0 + \frac{z}{r^2}(x^2 + y^2)}, \tag{1}$$

where λ is the wavelength of the light, x and y are the coordinate distribution of the conical lens respectively, f_0 is the initial focal length, z is the focal depth, c is the radial coordinate of the conical lens, $c = \sqrt{x^2 + y^2}$, and r is the radius of the conical lens. When a conical lens is used in the system, the image can be seen clearly in a large focal depth. In the proposed system, the LCoS is used to record the phase information of the conical lens. According to Eq. (1), the phase can be calculated and loaded on the LCoS. So,

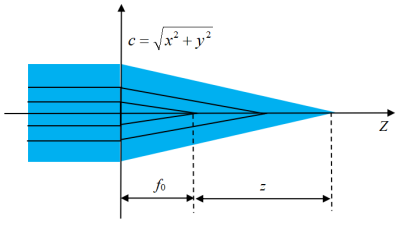

FIGURE 2. Principle of the conical lens.

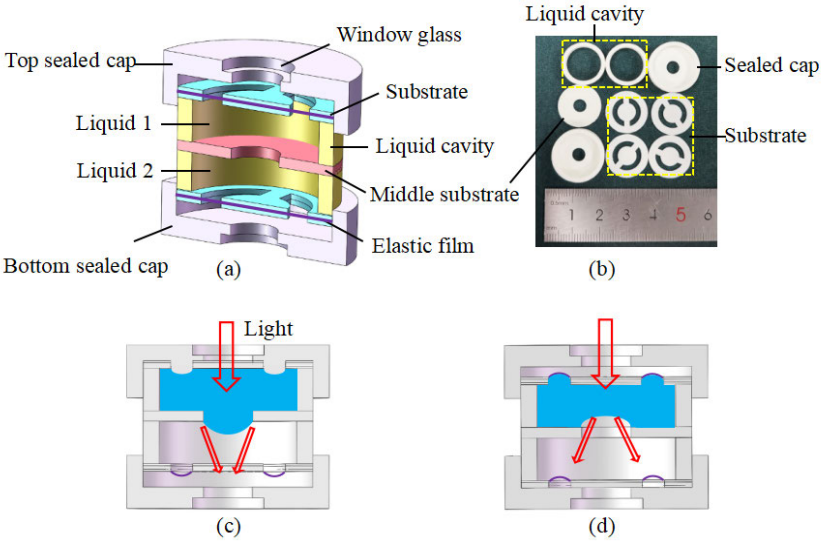

FIGURE 3. Structure and mechanism of the liquid lens. (a) Structure of the liquid lens; (b) elements of the liquid lens; (c) state-1 of the liquid lens; (d) state-2 of the liquid lens.

we can use the LCoS as a digital conical lens. By changing the parameters of the conical lens encoded on the LCoS, the function of an adjustable lens can be realized easily.

In order to realize zoom function, a liquid lens driven by mechanical mechanism is produced, as shown in Fig. 3. The cross-section of the liquid lens is shown in Fig. 3(a). The liquid lens consists two sealed caps, four substrates, one middle substrate, two elastic film and two window glasses. There is a hole in the middle substrate for forming the liquid-liquid interface due to the so-called mechanical-wetting effect. The elastic film is sandwiched between the two substrates. Liquid-1 and liquid-2 are filled in the liquid cavities, respectively. The elements of the liquid lens are also shown in Fig. 3(b). When the top sealed cap moves towards the substrate by rotating its own thread, the elastic film will be actuated due to the pneumatic pressure. Then the shape of the liquid-liquid interface is changed to form a convexity shape, as shown in state-1 of Fig. 3(c). In this state, the liquid lens can be used as a positive lens. In a similar way, when the bottom sealed cap moves towards the substrate, the shape of the liquid-liquid interface is changed from the convex shape to concave shape, as shown in state-2 of Fig. 3(d). In this state, the liquid lens works as a negative lens. The change of the liquid-liquid interface depends on the liquid surface tension and the applied liquid pressure, which can be described by the following Laplace equation:

$$P = \frac{2\gamma}{R}, \tag{2}$$

where P is the liquid pressure, γ is the liquid-liquid surface tension, and R is the curvature of the liquid-liquid interface. From Eq. (2) we can see that the curvature can be adjusted by changing the hydraulic pressure.

In the liquid lens, the top/bottom cap stays in its original state when the bottom/top cap moves, and the two caps cannot move simultaneously. This is due to the special mechanical structure of the liquid lens. For details, on each of the sealed caps, there is a pillar-like microstructure which can squeeze and deform the elastic film. When the top sealed cap moves, the elastic film in the bottom cavity can form a concave surface due to the hydraulic drive, as shown in Fig. 3(c). If the two sealed caps move at the same time, the liquids filled in the liquid cavities may be affected by the hydraulic pressure of the upper and lower chambers, which will not only damage the device, but also change the shape of the liquid-liquid interface slightly.

Compared with the electronic controlled liquid lens, the proposed liquid lens does not require the external drive systems or instruments. It can be driven just by rotating the sealed caps by our fingers. That is to say, the liquid lens requires almost no power. The affective imaging area of the proposed liquid lens is 5 mm, which is equal to or greater than that of the commercial liquid lenses. While, the cost of fabricating the device is very low, requiring only a few dozen grams of photosensitive resin. Therefore, the holographic system based on this kind of liquid lens can realize the low-cost function and is expected to be popularized commercially.

In the holographic reconstruction, when the collimated beam is used to illuminate the LCoS, the diffraction at the distance of l from the SLM can be expressed as the following formula:

$$U_l(u,v) = \frac{e^{ikl}}{i\lambda l}\exp[\frac{i\pi}{l\lambda}(u^2+v^2)]\int\int_{-\infty}^{\infty} \{U(x,y)\exp[\frac{ik}{2l}(x^2+y^2)]\}\exp[\frac{-2i\pi}{l\lambda}(xu+yv)]dxdy, \tag{3}$$

where $U_l(u,v)$ is the diffraction distribution of the reconstruction, $k = 2\pi/\lambda$, $U(x,y)$ is the distribution of the hologram and λ is the wavelength. When a digital conical lens with the focal length f_0 and focal depth z is loaded on the LCoS, the final phase distribution of the hologram can be expressed

as follows:

$$\phi'(x, y) = \phi(x, y) + \phi_c, \tag{4}$$

where $\varphi'(x, y)$ is the final phase distribution of the hologram, and $\varphi(x, y)$ is the phase distribution of the original object.

Since the phase of the digital conical lens is only added to that of the original object, the reproduced image can be separated from the zero-order light caused by the pixel structure of the LCoS. Then the diffracted image is modulated by the digital conical lens. When the diffracted image passes through the liquid lens, the final reproduced image on the receiving screen can be seen by adjusting the focal lengths of the liquid lens and digital conical lens simultaneously. Besides, due to the size of the liquid lens, the zero-order light and high-order light can be eliminated so that the reconstructed image can be displayed with a good quality. The modulation of the liquid lens can be calculated according to the following formula:

$$\frac{1}{l_2} + \frac{1}{l_1 - l_0} = \frac{1}{f_l}, \tag{5}$$

where l_0 is the position of the diffracted image reappeared clearly after passing through the conical lens, l_1 is the distance between the LCoS and the liquid lens, l_2 is the distance between the liquid lens and the receiving screen, and f_l is the focal length of the liquid lens. When $z = 0$, $l_0 = f_0$. In this case, when the focal length of the two zoom lenses is fixed, the reproduced image can only be seen at the fixed position of the receiving screen. Then size of the reconstructed image s can be calculated by the following equation:

$$s = \frac{f_0 \lambda l_2}{p(f_0 - l_1)}, \tag{6}$$

where p is the pixel size of the LCoS.

When $z > 0$, l_0 f_0. The diffracted image is modulated by the digital conical lens and it will first show a clear image in the depth range. In this case, when the focal length of the two zoom lenses is fixed, the reproduced image can be seen clearly even if the position of the receiving screen is moved. In the holographic projection, by changing the focal length of the digital conical lens and the liquid lens, the size of the reproduced image can be changed easily.

III. EXPERIMENTS AND RESULTS

The optical experiment is built in order to verify the effectiveness of the proposed system. The wavelength of the laser used in the experiment is 532 nm with the model of MGL-III-532. The focal length of the solid lens is 250 mm. The transmission and size of the BS are 80% and 25.4 mm×25.4 mm×25.4 mm, respectively. The pixel size of the LCoS is 6.4 μm and the resolution is 1920 × 1080. The distance between the LCoS and the liquid lens is 15 cm. The receiving screen is placed 25 cm behind the liquid lens in the initial situation. All the elements of the liquid lens are fabricated by a 3D printer (type of E3 @ JGAURORA, China). The elastic film is made from polydimethylsiloxane (PDMS) with a thickness of 200 μm (tensile strength: 5.0 Mpa; elasticity modulus: 2.3 Mpa). The diameters and heights of the sealed cap, liquid cavity, substrate, and middle substrate are 18.0 mm×5.0 mm, 10.0 mm×4.0 mm, 16.0 mm×0.5 mm, and 16.0 mm×1.0 mm, respectively. The diameter of the hole in the middle substrate is 5.0 mm. The phenylmethyl silicone oil (the density is 1.08 g/cm^3, the refractive index is 1.48) is used as liquid 1. The NaCl solution is used as liquid 2 (the density of the solution is 1.08 g/cm^3, the refractive index is 1.36). The densities of the filled liquids in the cavities are matched. Hence the liquid lens can have a reasonable mechanical stability.

1) OPTICAL PROPERTIES OF THE LIQUID LENS

In the initial state, the focal length of the liquid lens is measured to be ∼350 mm, as depicted in Fig. 4(a). The two sealed caps can be moved by rotating the screw thread inside the caps. The screw pitch is designed to be 0.2 mm. When the top sealed cap moves a distance of 0.8 mm, and 2.0 mm, the curvature of the liquid-liquid interface is changed accordingly, then the focal length of the liquid lens will be changed from ∼140 mm to ∼60 mm respectively, as shown in Figs. 4(b)-4(c). When we restore the top sealed cap to its original position and drive the bottom sealed cap to move a distance of 0.8 mm and 2.0 mm, the focal length can be changed from ∼−280 mm to ∼−70 mm respectively, as shown in Figs. 4(d)-4(f).

FIGURE 4. Experiment results of the liquid lens. (a) Initial state; (b) state when the top sealed cap moves 0.8 mm; (c) state when the top sealed cap moves 2.0 mm; (d) state when the bottom sealed cap moves 0.8 mm; (e) state when the bottom sealed cap moves 2.0 mm.

We also measured the focal length changes when the top sealed caps or bottom sealed cap moves, as shown in Fig. 5. From Fig. 5 we can see that when the top sealed cap moves a distance from 0 mm to 2.0 mm, the focal length can be tuned from ∼350 mm to ∼60 mm. And when the bottom sealed cap moves a distance from 0 mm to 2.0 mm, the focal length can be tuned from ∼350 mm to $+\infty$ and $-\infty$ mm to ∼−70 mm. The diameter of the liquid lens is 18.0 mm,

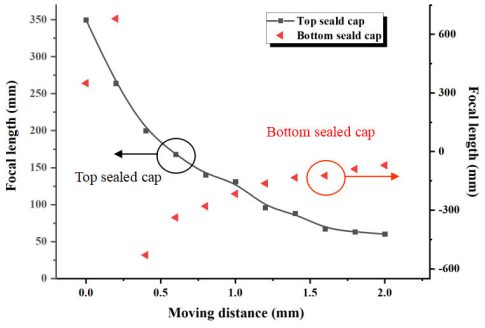

FIGURE 5. Focal length changes when the top sealed cap or bottom sealed cap moves.

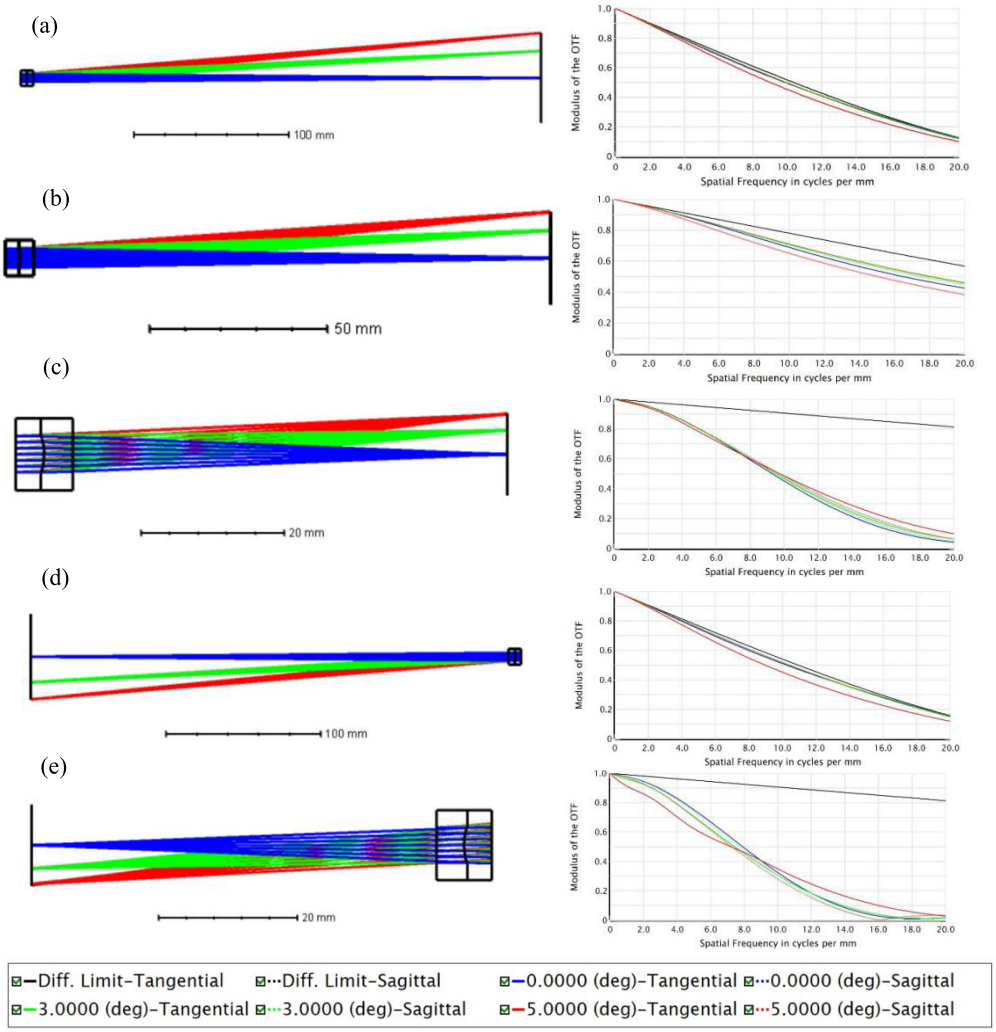

FIGURE 6. MTF properties of the liquid lens. (a) Initial state; (b) $f_l = 140$ mm; (c) $f_l = 60$ mm; (d) $f_l = -280$ mm; (e) $f_l = -70$ mm.

while the effective imaging area is 5 mm. Thus, when the images are captured by the CCD camera, there is a vignette effect obviously. The vignette effect is just the middle substrate. The simulated modulation transfer function (MTF) properties of the liquid lens at several focusing steps are shown in Fig. 6. The simulation and experimental results basically agree.

2) EXPERIMENTS OF THE HOLOGRAPHIC SYSTEM

In the experiment, the hologram of the recorded object is generated by the iterative Fourier transform algorithm [8]. A 'duck' is used as the recorded object and the hologram is generated. Firstly, to verify the function of the digital conical lens, only the receiving screen is placed behind the LCoS and the liquid lens is not used in the system. Then, a digital lens with the same focal length is used for the experimental comparison. The focal lengths of the digital conical lens and digital lens are both 500 mm. The focal depth of the digital conical lens is set to be 100 mm. The distance between the LCoS and receiving screen is set to be 500 mm, 550 mm and 600 mm, respectively. The multi-diffraction light and images exists in the reproduced image. Figs. 7(a)-7(c) are the first-order images by using the digital conical lens and

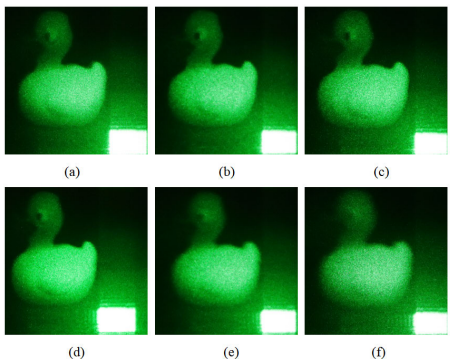

FIGURE 7. Results of the reconstructed images with different lenses. (a)-(c) Results by using the digital conical lens when the distance between the LCoS and receiving screen is set to be 500 mm, 550 mm and 600 mm, respectively; (d)-(f) results by using the digital lens when the distance between the LCoS and receiving screen is set to be 500 mm, 550 mm and 600 mm, respectively.

Figs. 7(d)-7(f) are the first-order images by using the digital lens. It can be seen that when the position of the receiving screen is moved, the zero-order light keeps unchanged. So, the reconstructed image can be separated from the zero-order light easily by using the digital conical lens. From the result we can see that the reconstructed images are clear when the receiving screen is placed at the focal plane of the two digital lenses respectively. When the receiving screen is moved away from the focal plane, the reconstructed images by using the digital lens appear to be blurred, while the reconstructed images by using the digital conical lens appear to be clear. So, by using the conical lens, the reconstructed image can be displayed clearly with a large focal depth.

Then the proposed system is conducted for the experiment. To verify that the proposed system has the advantages of large focal depth and undesirable light elimination, the focal length and focal depth of the digital conical lens are set to be 500 mm and 300 mm, respectively. When the distance between the liquid lens and receiving screen is 250 mm, the reconstructed image can be seen clearly by adjusting the focal length of the liquid lens, as shown in Fig. 8(a). Then the focal length of the liquid lens is kept unchanged. When the position of the receiving screen is moved 50 mm and 100 mm away, the reconstructed image by using the proposed system is still clear, as shown in Figs. 8(b)-8(c). At the same time, the zero-order diffraction light is eliminated due to the size of the liquid lens. Then the quality of the reconstructed image is improved compared with that of Fig. 7. That is, by using the proposed system, the digital conical lens can separate the zero-order light from the diffracted image, and the liquid lens can act as an aperture to eliminate the zero-order light in addition to being a zoom lens.

FIGURE 8. Result of the proposed system when the position of the receiving screen changes. (a) Result when the distance between the LCoS and receiving screen is 250 mm; (b) result when the distance between the LCoS and receiving screen is 300 mm; (c) result when the distance between the LCoS and receiving screen is 350 mm.

Moreover, the traditional zoom system by using the liquid lens and the digital lens is used for comparison. The focal length of the digital lens is set to be 500 mm. The focal lengths of the digital lens and liquid lens is kept unchanged. As shown in Fig. 9, it can be seen clearly that the reconstructed image by using the traditional system becomes blurred when the position of the receiving screen is moved.

Then the experiment is performed to verify that the proposed system has the advantages of zoom function. When the positions of the LCoS, liquid lens and receiving screen keep unchanged, holographic zoom function can be realized

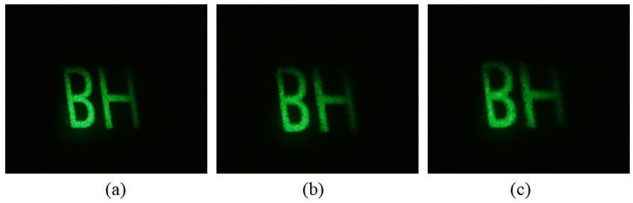

FIGURE 9. Results of the traditional system when the position of the receiving screen changes. (a) Results when the distance between the LCoS and receiving screen is 250 mm; (b) results when the distance between the LCoS and receiving screen is 300 mm; (c) results when the distance between the LCoS and receiving screen is 350 mm.

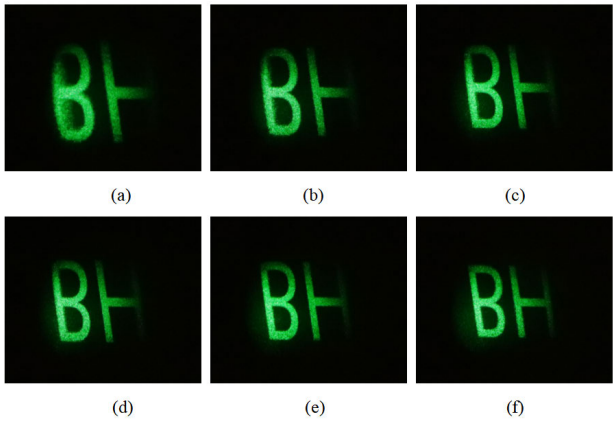

FIGURE 10. Results of the reconstructed image when the position of the receiving screen is kept unchanged. (a) $f_0 = 300$ mm; (b) $f_0 = 400$ mm; (c) $f_0 = 500$ mm; (d) $f_0 = 550$ mm; (e) $f_0 = 650$ mm; (f) $f_0 = 900$ mm.

by changing the focal lengths of the liquid lens and digital conical lens simultaneously. The results are shown in Fig. 10. According to Eqs. (3)-(5), the relationship between the focal lengths of the liquid lens and digital conical lens can be calculated easily. Figs. 10(a)-10(f) are the reconstructed images when the focal lengths of the digital conical lens ranges from 300 mm to 900 mm. It can be seen clearly that the size of the reconstructed images can be adjusted easily by controlling the focal lengths of the two adjustable lenses simultaneously. However, when the magnification increases to a certain extent, only part of the reproduced image can be seen due to the aperture limitation of the liquid lens, as shown in Fig. 10(a). Since the digital conical lens has a higher spatial frequency when the focal length decreases, the minimum value of f_0 is set to be larger than 250 mm in the experiment according to the Nyquist sampling theorem. The magnification of the reconstructed image is recorded to be 1 when the focal length of the digital conical lens is set to be 650 mm. The focal depth is set to be 300 mm. By adjusting the focal lengths of the liquid lens and the digital conical lens, we record the size of the reproduced image at its clearest. The relationship between the magnification M and the focal length of the digital conical lens in the proposed system is shown in Fig. 11. From the results we can see that the magnification of the proposed system is increased as the focal length of the digital conical lens decreases.

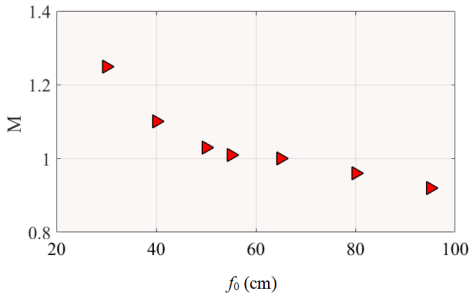

FIGURE 11. Relationship between the magnification and the focal length of the digital conical lens.

In the proposed system, the green color laser is used for the experiments. By adjusting the focal lengths of the two adjustable lenses, holographic zoom reproduction can be realized easily without moving any components. At the same time, the zero-order diffraction light can be separated and eliminated completely. So, the holographic zoom projection with a good quality can be achieved. In addition, the reconstructed image can be displayed with a large focal depth. That is, even if the position of the reproduced image changes, a clear reproduced image can be seen at a certain focal depth. The holographic images can be projected on any location or with any size according to the requirement. So, the proposed system has the unique advantages such as large focal depth, zoom function and high quality compared with the traditional systems.

IV. APPLICATIONS

A. AR DISPLAY

Due to the unique advantages of the proposed system, it can be used in the AR display. To verify the feasibility of the AR display, a BS prism is added at the end of the reproduction light path. When the reconstructed image passes through the BS, it can be reflected. Besides, a 'beer' is placed in the transmission direction of the BS. A 'cube' is used for the holographic reconstruction, and a CCD camera is used to capture the reconstructed image. In the experiment, by adjusting the focal lengths of the liquid lens and the digital conical lens, the position of the reproduced image of the 'cube' can be adjusted to the same depth as the 'bear', as shown in Fig. 12(a). In this state, we can see both the real object 'bear' and the holographic reproduced image 'cube' at the same time. So, the proposed system can be used in the holographic AR display. Then the focal lengths of the liquid lens and the digital conical lens are kept unchanged. Due to the large focal depth of the digital conical lens, the holographic reproduced image can also be seen clearly at different depths, as shown in Fig. 12(b). In this state, the holographic reconstructed image is clear, while the real object 'bear' becomes blurred.

As shown in Fig. 12, the feasibility and the large focal depth that the proposed system is used in the holographic AR display are proved. Then another experiment is performed to verify the zoom function of the holographic AR display.

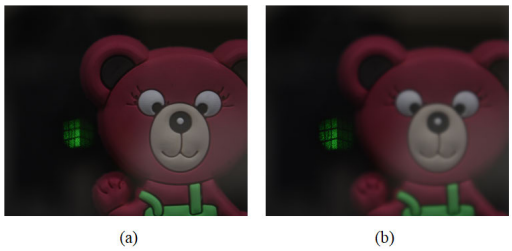

FIGURE 12. Results of holographic AR display when (a) the depths of the reconstructed image and the 'bear' are the same, and (b) the depth of the reconstructed image changes.

In this experiment, in order to realize the zoom function, the focal lengths of the liquid lens and the digital conical lens are adjusted at the same time. The results are shown in Fig. 13, where Fig. 13(a) is the result in the initial state and Fig. 13(b) is the result when the reconstructed image is magnified. So, we can see that zoom function can be also realized easily when the proposed system is used for holographic AR display.

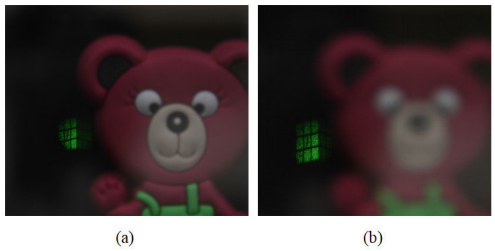

FIGURE 13. Zoom results of the holographic AR display (a) in the initial state and (b) when the reconstructed image is magnified.

Compared with the traditional holographic AR display systems such as [22], the proposed system can not only achieve the effect of AR display, but also have the large focal depth and zoom function. The volume of the system is reduced significantly. In addition, the proposed liquid lens is driven by rotating the top/bottom cover of our finger, rather than by the driving system. The electrowetting-driven liquid lenses and other mechanically-driven liquid lenses often require AC/DC regulated power supplies or syringe pumps. Therefore, they are not suitable be applied in the real holographic display. The simple structure and ease of driving mechanism are just the reason why it can be applied in real application. In the future, it is expected to be further integrated and truly applied to the holographic near-eye display.

B. COLOR HOLOGRAPHIC ZOOM SYSTEM

In the color holographic reproduction, the size and position of the reconstructed image are different due to the different wavelengths of the three color lasers. Therefore, the magnification chromatic aberration and axial chromatic aberration exist in the reproduced image, as shown in Fig. 14. In the proposed system, the size and the depth of the reconstructed image can be adjusted easily. So, the proposed system is

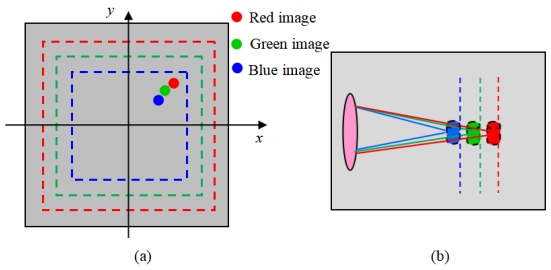

FIGURE 14. Chromatic aberration in the holographic system. (a) Magnification chromatic aberration; (b) axial chromatic aberration.

also expected to be applied to the color holographic zoom display without the color chromatic aberration. Here we give the scheme of the color holographic zoom system, as shown in Fig. 15. Each of the three color lasers illuminates one third area of the LCoS after passing through the mirror and BSs, respectively. Then the diffraction image passes through the BS and liquid lens, and the reconstructed image can be seen on the receiving screen.

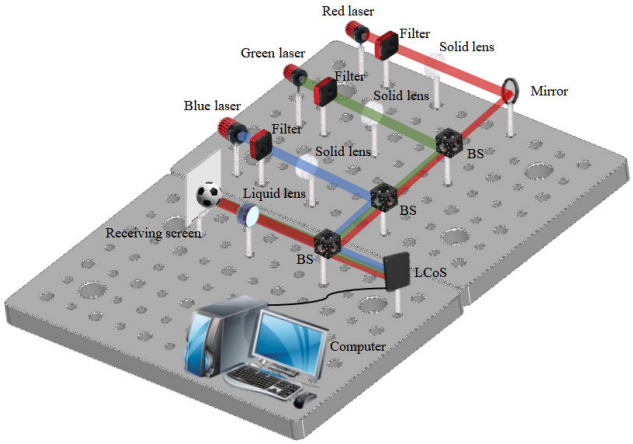

FIGURE 15. Structure of the color holographic zoom system.

From the above analysis, we know that the reproduced image can be adjusted by changing the focal lengths of the adjustable lenses. In the color holographic system, the holograms of three different digital conical lenses are loaded on those of the three color objects respectively. By setting the focal depth of the digital conical lens, the three color reconstructed images can be clearly seen on the receiving screen. Thus, the axial chromatic aberration of Fig. 14(a) can be eliminated easily. Besides, the reconstructed image can also be seen clearly even if the receiving screen is moved, as shown in Fig. 8. On the other hand, by adjusting the focal lengths of the two adjustable lenses at the same time, the sizes of the color reconstructed images can be adjusted conveniently. For the magnification chromatic aberration, the color reproduced image sizes of the three colors can be kept the same by pre-scaling the components of the three colors. Therefore, the three color images can be reproduced with the same size. Thus, the magnification chromatic aberration can be eliminated easily.

When the proposed system is applied to color holographic display, it can not only eliminate the color chromatic aberration, but also has the characteristics of zoom function and large depth. In addition, the undesirable light in the reproduced image can also be eliminated. So, the proposed color system has unique advantages compared with the traditional color holographic system.

In the experiment, in order to prove the zoom effect of the proposed system, the distance between the LCoS and the liquid lens is set as 15 cm for example. The distance can be set according to the actual requirements. In fact, the proposed system is more conducive to the implementation of compact systems. The closer the liquid lens is to the SLM, the more light passes through the liquid lens and the brighter the reconstructed image will be.

In the experiment, the calculation speed of the hologram can not meet the requirement of the real-time display. In the future, we can try other algorithms, or use a parallel computing platform to achieve the rapid hologram generation. Compared with the traditional lens, the image energy of the digital conical lens will be reduced. In the focal depth range, the power remains unchanged. The smaller the focal depth is, the higher the energy is. In the proposed system, the digital conical lens can greatly expand the reconstruction range, although it will weaken the reconstructed image. Therefore, we make a balance between the energy and other properties. By choosing the corresponding parameters, the high resolution can be obtained and the scope of the holographic reconstruction can be expanded, instead of restricting the reconstructed image to the back focal plane of the spherical lens. In our experiment, we mainly study the zoom effect and depth reproduction of the proposed system. In the future, we will further study the energy distribution of the digital conical lens and hope to optimize the corresponding parameters to achieve the best holographic zoom effect. We believe the proposed system can bring new ideas to the development of holographic technology.

V. CONCLUSIONS

In this paper, a holographic zoom system based on two adjustable lenses is proposed. The adjustable lenses are used as the core components of the proposed system, where the liquid lens with special structure is designed and produced by the 3D printer. By mechanically controlling the curvature of the liquid-liquid surface, the focal length of the liquid lens can be changed easily. As another adjustable lens, the digital conical lens can not only separate the zero-order light, but also adjust the focus and depth. The experiment results show that the size and depth of the reconstructed image can be changed easily. Moreover, the zero-order light can also be eliminated with such a simple system. The proposed system is expected to be applied to the systems such as color projection and multi-layer display.

REFERENCES

[1] K. Wakunami, P.-Y. Hsieh, R. Oi, T. Senoh, H. Sasaki, Y. Ichihashi, M. Okui, Y.-P. Huang, and K. Yamamoto, "Projection-type see-through holographic three-dimensional display," *Nature Commun.*, vol. 7, no. 1, Dec. 2016, Art. no. 12954.

[2] H. Zhang, L. Li, D. L. McCray, D. Yao, and A. Y. Yi, "A microlens array on curved substrates by 3D micro projection and reflow process," *Sens. Actuators A, Phys.*, vol. 179, pp. 242–250, Jun. 2012.

[3] J. Park, K. Lee, and Y. Park, "Ultrathin wide-angle large-area digital 3D holographic display using a non-periodic photon sieve," *Nature Commun.*, vol. 10, no. 1, Dec. 2019, Art. no. 1304.

[4] P.-A. Blanche, A. Bablumian, R. Voorakaranam, C. Christenson, W. Lin, T. Gu, D. Flores, P. Wang, W.-Y. Hsieh, M. Kathaperumal, B. Rachwal, O. Siddiqui, J. Thomas, R. A. Norwood, M. Yamamoto, and N. Peyghambarian, "Holographic three-dimensional telepresence using large-area photorefractive polymer," *Nature*, vol. 468, no. 7320, pp. 80–83, Nov. 2010.

[5] H. Yu, K. Lee, J. Park, and Y. Park, "Ultrahigh-definition dynamic 3D holographic display by active control of volume speckle fields," *Nature Photon.*, vol. 11, no. 3, pp. 186–192, Mar. 2017.

[6] T. Shimobaba, M. Makowski, T. Kakue, M. Oikawa, N. Okada, Y. Endo, R. Hirayama, and T. Ito, "Lensless zoomable holographic projection using scaled fresnel diffraction," *Opt. Express*, vol. 21, no. 21, pp. 25285–25290 Oct. 2013.

[7] I. Ducin, T. Shimobaba, M. Makowski, K. Kakarenko, A. Kowalczyk, J. Suszek, M. Bieda, A. Kolodziejczyk, and M. Sypek, "Holographic projection of images with step-less zoom and noise suppression by pixel separation," *Opt. Commun.*, vol. 340, pp. 131–135, Apr. 2015.

[8] Y. Su, Z. Cai, L. Shi, F. Zhou, H. Chen, and J. Wu, "Magnified holographic projection based on spatial light modulators," *Opt. Appl.*, vol. 48, no. 4, pp. 589–600, 2018.

[9] F.-J. Gan, D. Wang, C. Wang, J. Wang, and Q.-H. Wang, "A method of holographic magnification based on fresnel diffraction," *J. Soc. Inf. Display*, vol. 24, no. 6, pp. 355–359, Jun. 2016.

[10] D. Wang, C. Liu, L. Li, X. Zhou, and Q.-H. Wang, "Adjustable liquid aperture to eliminate undesirable light in holographic projection," *Opt. Express*, vol. 24, no. 3, pp. 2098–2105, Feb. 2016.

[11] C. Chang, J. Wu, Y. Qi, C. Yuan, S. Nie, and J. Xia, "Simple calculation of a computer-generated hologram for lensless holographic 3D projection using a nonuniform sampled wavefront recording plane," *Appl. Opt.*, vol. 55, no. 28, pp. 7988–7996, Oct. 2016.

[12] H. Ren and S.-T. Wu, "Variable-focus liquid lens," *Opt. Express*, vol. 15, no. 10, pp. 5931–5936, May 2007.

[13] C. Liu, D. Wang, and Q.-H. Wang, "Variable aperture with graded attenuation combined with adjustable focal length lens," *Opt. Express*, vol. 27, no. 10, pp. 14075–14084, May 2019.

[14] B. Jin, H. Ren, and W.-K. Choi, "Dielectric liquid lens with chevron-patterned electrode," *Opt. Express*, vol. 25, no. 26, pp. 32411–32419, Dec. 2017.

[15] X. Shen, Y.-J. Wang, H.-S. Chen, X. Xiao, Y.-H. Lin, and B. Javidi, "Extended depth-of-focus 3D micro integral imaging display using a bifocal liquid crystal lens," *Opt. Lett.*, vol. 40, no. 4, pp. 538–541, Feb. 2015.

[16] A. Hassanfiroozi, Y.-P. Huang, B. Javidi, and H.-P.-D. Shieh, "Dual layer electrode liquid crystal lens for 2D/3D tunable endoscopy imaging system," *Opt. Express*, vol. 24, no. 8, pp. 8527–8538, Apr. 2016.

[17] P.-Y. Chou, J.-Y. Wu, S.-H. Huang, C.-P. Wang, Z. Qin, C.-T. Huang, P.-Y. Hsieh, H.-H. Lee, T.-H. Lin, and Y.-P. Huang, "Hybrid light field head-mounted display using time-multiplexed liquid crystal lens array for resolution enhancement," *Opt. Express*, vol. 27, no. 2, pp. 1164–1177, Jan. 2019.

[18] H.-C. Lin, N. Collings, M.-S. Chen, and Y.-H. Lin, "A holographic projection system with an electrically tuning and continuously adjustable optical zoom," *Opt. Express*, vol. 20, no. 25, pp. 27222–27229, Dec. 2012.

[19] K. Mishra, A. Narayanan, and F. Mugele, "Design and wavefront characterization of an electrically tunable aspherical optofluidic lens," *Opt. Express*, vol. 27, no. 13, pp. 17601–17609, 2019.

[20] N. Hasan, H. Kim, and C. H. Mastrangelo, "Large aperture tunable-focus liquid lens using shape memory alloy spring," *Opt. Express*, vol. 24, no. 12, pp. 13334–13342, Jun. 2016.

[21] H. Ren, D. Fox, P. A. Anderson, B. Wu, and S.-T. Wu, "Tunable-focus liquid lens controlled using a servo motor," *Opt. Express*, vol. 14, no. 18, pp. 8031–8036, 2006.

[22] M.-S. Chen, N. Collings, H.-C. Lin, and Y.-H. Lin, "A holographic projection system with an electrically adjustable optical zoom and a fixed location of zeroth-order diffraction," *J. Display Technol.*, vol. 10, no. 6, pp. 450–455, Jun. 2014.

[23] J. S. Lee, Y. K. Kim, and Y. H. Won, "Time multiplexing technique of holographic view and Maxwellian view using a liquid lens in the optical see-through head mounted display," *Opt. Express*, vol. 26, no. 2, pp. 2149–2159, Jan. 2018.

DI WANG is a Postdoctoral Research Fellow of optics with the School of Instrumentation and Optoelectronic Engineering, Beihang University. She has published more than 40 articles. Her current research interest includes information display technologies.

CHAO LIU is a Postdoctoral Research Fellow of instrumentation with the School of Instrumentation and Optoelectronic Engineering, Beihang University. He has published more than 40 articles. His current research interests include optical system design, liquid lens, and information displays.

NAN-NAN LI is currently pursuing the M.S. degree in with the School of Electronics and Information Engineering, Sichuan University. His current research interest includes information displays.

QIONG-HUA WANG received the M.S. and Ph.D. degrees from the University of Electronic Science and Technology of China (UESTC), in 1995 and 2001, respectively. She was a Professor with the School of Electronics and Information Engineering, Sichuan University, from 2004 to 2018. She was a Postdoctoral Research Fellow with the School of Optics/CREOL, University of Central Florida, from 2001 to 2004. She worked at the UESTC, from 1995 to 2001. She is a Professor of optics with the School of Instrumentation Science and Opto-Electronics Engineering, Beihang University. She published approximately 200 articles cited by science citation index and authored two books. She holds five U.S. patents and 90 Chinese patents. Her research interests include optics and optoelectronics, especially display technologies. She is a Fellow of the Society for Information Display and an Associate Editor of *Optics Express* and the *Journal of the Society for Information Display*.